Influence of Sapwood and Heartwood on *Cryptomeria japonica* Toughness Mechanism in Mode-I Radial-longitudinal and Tangential-longitudinal Systems

Tatiana Mitie Enta [a,b,*] Arata Yoshinaga [b] Norihiko Yamada [b] and Koji Murata [b]

** Corresponding author: tatianaenta@gmail.com*

DOI: 10.15376/biores.21.2.3894-3909

GRAPHICAL ABSTRACT

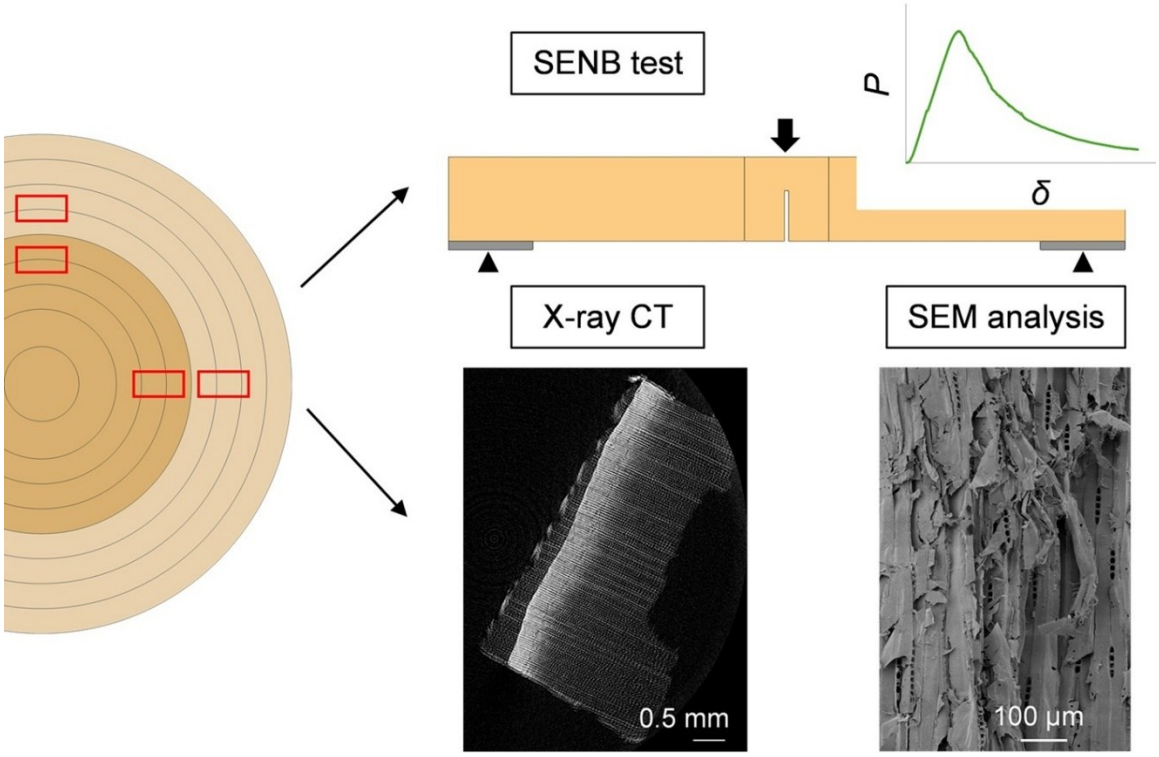

Influence of Sapwood and Heartwood on *Cryptomeria japonica* Toughness Mechanism in Mode-I Radial-longitudinal and Tangential-longitudinal Systems

Tatiana Mitie Enta [a,b,*] Arata Yoshinaga [b] Norihiko Yamada [b] and Koji Murata [b]

The influence of sapwood and heartwood on many mechanical properties has been studied; however, their influence on fracture mechanics remains unclear. This study investigated the influence of sapwood and heartwood on the toughness mechanism of *Cryptomeria japonica* in mode-I radial-longitudinal (RL) and tangential-longitudinal (TL) systems. A single-end-notched bending test was performed to obtain the fracture toughness of four specimen types: RSW, RHW, TSW, and THW (where R = RL system, T = TL system, SW = sapwood, and HW = heartwood). Thereafter, X-ray computed tomography and scanning electron microscopy (SEM) analyses were performed to evaluate the fracture at the microscale level. For all properties evaluated, the RL system showed the highest values, and within the same system, sapwood had the highest values. However, the statistical analysis concluded that fracture toughness was the only property with a significant difference for all specimen types. Microscale analyses using SEM revealed that the higher toughness mechanism values found in the sapwood specimens were related to higher proportions of cell fracture than those in other specimen types. This implies that the toughness mechanism may depend on the fracture of microstructural tissues.

DOI: 10.15376/biores.21.2.3894-3909

Keywords: Sugi; Fracture mechanics; Fracture energy; Fracture toughness; RL; TL

*Contact information: a: Ph.D. student; b: Division of Forest and Biomaterials Science, Graduate School of Agriculture, Kyoto University, Kyoto, Japan; *Corresponding author: tatianaenta@gmail.com*

INTRODUCTION

Wood is widely used as an engineering material. It is known for its relatively low density, good mechanical properties, and versatility. However, because wood is a strongly anisotropic material, it is weak against loads perpendicular to the longitudinal direction, and special care must be taken concerning its cleavage strength. Nonetheless, according to Jeromidis (1980), the ability of wood to combine stiffness and strength with high resistance to crack propagation is a feature that deserves attention.

Among the fracture modes, mode-I, also known as the opening mode, is the critical mode for most structural materials; hence, it has received considerable attention (Smith *et al*. 2003). Crack propagation in wood, as in many other anisotropic materials, is influenced by the direction of crack growth (Jeronimidis 1980). Six main crack propagation systems exist, each composed of two letters, where the first letter indicates the direction perpendicular to the crack plane, and the second letter represents the crack propagation direction.

Most studies have focused on radial-longitudinal (RL) and tangential-longitudinal (TL) systems because cracks easily propagate along the grain (Smith *et al*. 2003). In these directions, wood behaves as a quasi-brittle material (Jeronimidis 1980). Wood loaded in mode-I exhibits greater fracture resistance in the RL system than in the TL system. This behavior has been previously reported in *Pinus radiata* (Boatright and Garrett 1983), *Picea abies*, *Pinus sylvestris* (Fonselius and Riipola 1992), and spruce (Tan *et al*. 1995).

When evaluating wood with different moisture contents (MC) and heat treatments, the same conclusion was reached by Majano-Majano *et al*. (2012) for *Fagus sylvatica* and *Fraxinus excelsior*. An increase in MC influenced the fracture energy (G_f) more than it influenced the fracture toughness (K_{IC}), also known as critical stress intensity; hence, more energy per unit area was required to split wood at a higher MC. Thus, the more severe the heat treatment, the greater the decrease in G_f and K_{IC} was observed in their study. In addition, Merhar *et al*. (2023) evaluated the effects of MC and thermal treatments on *P. abies* and found a positive relationship between the strain energy release rate and MC and a negative relationship with thermal modification and MC.

Moreover, a higher K_{IC} in the RL system than in the TL system for *F. sylvatica* was reported by Ozyhar *et al*. (2012). Increasing MC resulted in a decrease in the modulus of elasticity, strength, and K_{IC}. In addition, six species (hardwood and softwood) in the green state were analyzed by Özden *et al*. (2017), and the G_f in the RL system was 1.6 times greater. The RL system exhibited tough ductile failure behavior, and the TL was more brittle. Another study, which included both hardwood and softwood, was conducted by Reiterer *et al*. (2002). The study compared three hardwoods and one softwood and found a strong dependency of stiffness (k_{init}) and K_{IC} on density. The softwood showed stable crack propagation and a more ductile behavior, whereas the hardwoods presented unstable crack propagation and more linear elastic and brittle behaviors. All specimens had higher k_{init}, G_f, and K_{IC} values in the RL system. Higher ratios between the RL and TL systems k_{init} and K_{IC} were observed in hardwoods with higher ray percentages. G_f was higher in the RL system, but the same ratios between the RL and TL systems were not observed for this mechanical property, leading to the assumption that rays might play a more important role in the crack initiation phase than in the propagation phase.

Most studies have shown a superior wood-toughness mechanism in the RL system compared with that of the TL system. Nonetheless, research with different outcomes has also been reported. Accordingly, Majano-Majano *et al*. (2018) found the same G_f in the RL and TL systems of *Eucalyptus globulus*; however, the RL system had higher cohesive stress values at lower crack-tip opening displacements. Moreover, Frühmann *et al*. (2002) reported higher fracture energy for the *F. sylvatica* TL system. This result was attributed to the higher amount of latewood in the TL system specimens than in the RL system specimens, where earlywood was predominant. In addition, Matsumoto and Nairn (2012) reported similar initial toughness for Douglas-fir RL and TL systems. However, as the cracks propagated, the curves differed. The RL curve remained constant, and the TL toughness increased linearly as the crack grew. Furthermore, Romanowicz and Grygorczuk (2024) reported superior maximum load (P_{max}) and critical resistance values for *P. sylvestris* TL system. Although a higher cohesive strength was observed for the RL system, the difference was small.

The fracture difference between the systems is explained by the capacity of the rays to arrest or bridge propagating cracks in the RL system, thereby increasing K_{IC}. In contrast, in the TL system, the rays contribute to a reduction in K_{IC}, where the crack propagates along the least resistant paths caused by the rays (Smith *et al*. 2003). Another explanation

is that the typical fracture path in the RL system is cell fracture (intracellular fracture), in which a crack propagates through the secondary cell walls. Whereas in the TL system, it occurs mostly by cell separation (intercellular fracture), where propagation occurs through the middle lamella and primary cell wall (Conrad *et al*. 2003).

Although previous studies confirmed the higher resistance of RL systems to cracks, the influence of sapwood and heartwood has remained unclear. Furthermore, the influence of sapwood and heartwood on the other mechanical properties yielded different results. Merela and Čufar (2013) evaluated four mechanical properties of three species of the genus *Quercus* and found no significant difference between sapwood and heartwood. Nevertheless, according to Bektas *et al*. (2020), the differences between sapwood and heartwood physical and mechanical properties must be considered. Correspondingly, nine mechanical properties of *P. sylvestris*, *Pinus brutia*, *Populus usbekistanica*, and *Eucalyptus grandis* were investigated, and most properties had significant differences between sapwood and heartwood.

Sapwood and heartwood have the same cell structure, such as microfibril angle; however, their chemical composition differs, and more extractives, especially those of aromatic compounds, were found in the cell wall matrix of the heartwood (Song *et al*. 2014). Moreover, it was concluded that sapwood and heartwood have a considerable difference in their chemical composition (Bertaud and Holmbom 2004). Because the chemical composition influences the development of the fracture process zone (FPZ), this study aimed to evaluate the toughness mechanism to investigate whether there is a difference between *Cryptomeria japonica* sapwood and heartwood in mode-I RL and TL systems.

EXPERIMENTAL

To evaluate the mode-I toughness mechanism of *C. japonica*, popularly known as "sugi" in Japan, a single-edge notched bending (SENB) test was performed in the RL and TL systems using sapwood and heartwood separately. There were four specimen types with seven repetitions each, totalizing 28 specimens. To ensure the comparison between sapwood and heartwood, only mature and clear wood was included in the study. Owing to the size limitation of the sawn lumber, the specimens were composed of three parts glued with epoxy resin, and the longitudinal direction of the middle part was aligned with the loading direction (Fig. 1). The notch was made with a circular saw, and a starter notch of 1 mm was made with a razor blade to initiate the crack. The specimens were air-dried and posteriorly stored in a room without temperature and humidity control during summer for two months. For each specimen type, the middle parts were selected such that they had approximately equal densities (Table 1). The mean density of the entire specimen was 360 kg/m^3, and the MC was 16%. The values for each specimen type are shown in Table 1, and the dimensions of the specimens are shown in Fig. 1.

To obtain the k_{init}, G_f, P_{max}, and K_{IC}, the SENB test was performed in a material testing machine (Shimadzu, AGS-100 kN) with a 0.5 mm/min loading speed rate until the load dropped to 5 N. The testing machine was originally equipped with a 100 kN load cell; however, the experiment was carried out with a 5 kN load cell. The average temperature and humidity during the experiment were 24.3 °C and 79%, respectively. The variable k_{init} is proportional to the material stiffness and represents the deformation behavior before the crack starts. G_f represents the entire fracture process, including crack initiation and

propagation yield, until complete separation of the specimen, and is derived from the load-displacement curve. K_{IC} refers to the maximum stress that a material supports before crack initiation (Majano-Majano *et al*. 2012).

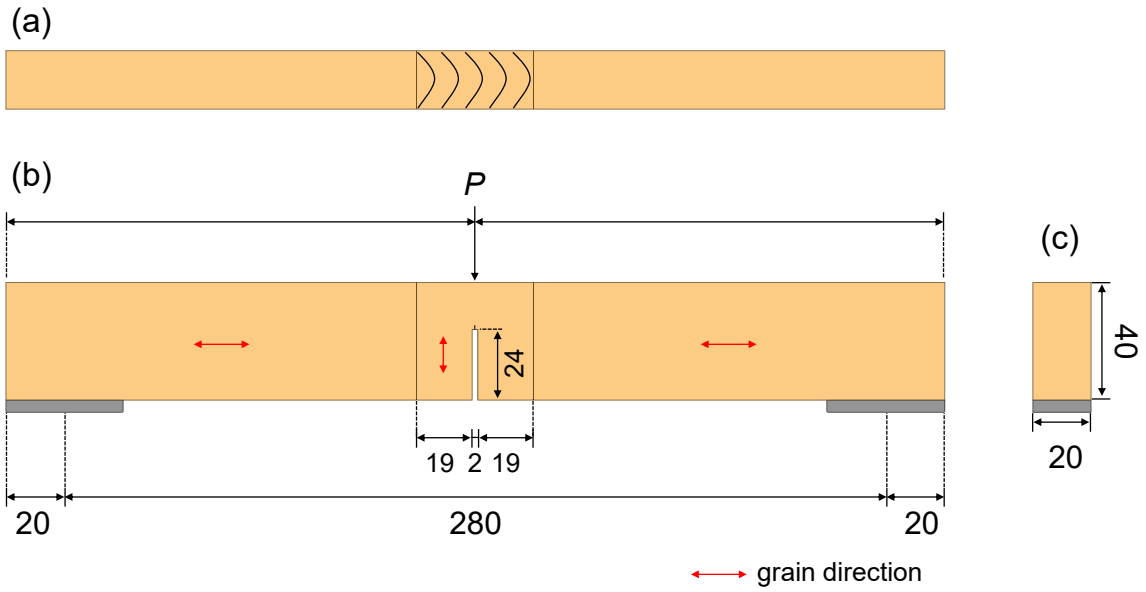

Fig. 1. Single-edge notched bending (SENB) test for radial-longitudinal (RL) specimen: (a) top, (b) front, and (c) lateral view

Table 1. Density and Moisture Content of Each Specimen Type in the Single-edge Notched Bending (SENB) Test

Specimen Type	Density* (kg/m^3)	CV (%)	MC (%)	CV (%)
RSW	357	0.1	15.2	2.0
RHW	355	0.2	16.2	1.7
TSW	369	1.1	14.1	1.8
THW	340	1.6	18.9	1.2

Note: R is the radial-longitudinal system, T is the tangential-longitudinal system, SW is the sapwood, and HW is the heartwood. *middle part density

The value of k_{init} was obtained from the initial slope of the load-displacement curve from 10 to 40% of P_{max}. G_f and K_{IC} were calculated according to Eqs. 1 and 2, respectively:

$$G_f = \frac{W}{A} \quad (1)$$

where G_f is the fracture energy (J/m^2), W is the total energy (J), and A the fracture area (m^2).

$$G_I = {K_{IC}}^2 \times \sqrt{\frac{{}^1/_{E_x} \times {}^1/_{E_y}}{2}} \times \left[\frac{{}^1/_{E_y}}{{}^1/_{E_x}} + 2\left(-\frac{\nu_{xy}}{E_x}\right) + \frac{1}{G_{xy}}\right]^{\frac{1}{2}} \quad (2)$$

In Eq. 2, G_I is the fracture release energy (J/m^2), K_{IC} is the fracture toughness (Pa·m$^{1/2}$), E is the modulus of elasticity (Pa), v is Poisson's ratio, G is the shear modulus (Pa), x is the crack propagation direction, and y is the direction perpendicular to the crack plane.

Equation 2 was obtained from Sih *et al*. (1965), and G_I was obtained using the virtual crack closure technique (VCCT) through three-dimensional Finite Element Analysis (FEA) using ANSYS Workbench Mechanical 2025 R1 software with the element type SOLID185. Finite element approaches to fracture mechanics can be classified as direct when the stress intensity factors are calculated directly from the solution, or indirect, when the energy release rate is calculated, and posteriorly when the stress intensity factor is derived from it (Rybicki and Kanninen 1977). Due to software limitations, in this work, the indirect method was adopted using the VCCT. VCCT was first introduced by Rybicki and Kanninen (1977) and has been broadly utilized for interfacial cracks to calculate the total and individual energy release rates, using the outcomes from a FEA (Xie *et al*. 2004). In this technique, it is assumed that for an infinitesimal crack opening, the released strain energy is equivalent to the work required to close the crack (Pietropaoli 2011).

The crack was modeled as a pre-meshed crack with a mesh around the crack of 1 mm. A load corresponding to each specimen's experimental P_{max} was applied to the models to obtain the G_I. The density was the average experimental value, and the orthotropic elasticity properties were obtained from Sawada (1963) (Table 2). Ideally, the material properties should have been obtained from experiments conducted by the authors. However, due to limited resources, that was not possible. Nevertheless, the majority of the studies found in the literature report K_{IC} results; therefore, K_{IC} values were included in this study for comparison purposes. Posteriorly, an analysis of variance (ANOVA) at a 1% significance level and Tukey tests were performed for all the variables evaluated.

To investigate the fracture mechanism at the microscopic level, X-ray computed tomography (CT) was performed on two specimens using ScanXmate-A080S (Voxel Works) at 40 kV. Thus, scanning electron microscopy (SEM) analysis was performed, in which the specimens were coated with gold using a JFC – IIOOE (JEOL, Tokyo, Japan) and examined in a JSM-6060 (JEOL) with an acceleration voltage of 5 kV. Sixteen specimens were used, with four specimens per type. To ensure reliable results, representative specimens were selected for both analyses.

Table 2. Finite Element Analysis (FEA): *Cryptomeria japonica* Material Properties

Material Property		Unit
Density	360	kg/m^3
Orthotropic Elasticity		
E_X	7500	N/mm²
E_Y	600	N/mm²
E_Z	300	N/mm²
ν_{XY}	0.41	
ν_{YZ}	0.90	
ν_{XZ}	0.60	
G_{XY}	625.5	N/mm²
G_{YZ}	15	N/mm²
G_{XZ}	352.5	N/mm²

In Table 2, E is the modulus of elasticity, ν is the Poisson's ratio, G is the shear modulus, X is the longitudinal direction, Y is the radial direction, and Z is the tangential direction.

RESULTS AND DISCUSSION

SENB Test

The RL system showed higher P_{max} values, and within the same system, sapwood showed higher values (Fig. 2 and Fig. 4a). The average P_{max} values for the RL system for sapwood (RSW), RL system for heartwood (RHW), TL system for sapwood (TSW), and TL system for heartwood (THW) were 51.2, 45.2, 31.8, and 24.9 N, respectively. The same behavior was observed for k_{init}, G_f, P_{max}, and K_{IC} (Figs. 3 and 4).

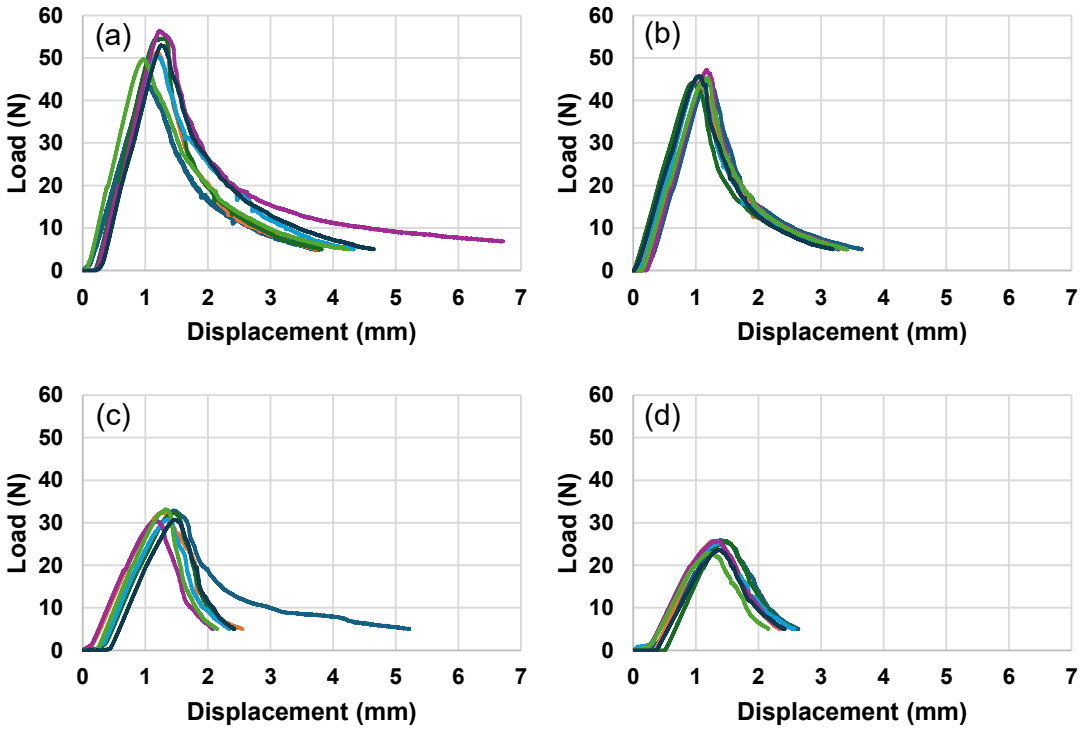

Fig. 2. Load-displacement curves. (a) Radial-longitudinal system for sapwood (RSW), (b) radial-longitudinal system for heartwood (RHW), (c) tangential-longitudinal system for sapwood (TSW), and (d) tangential-longitudinal system for heartwood (THW) specimens

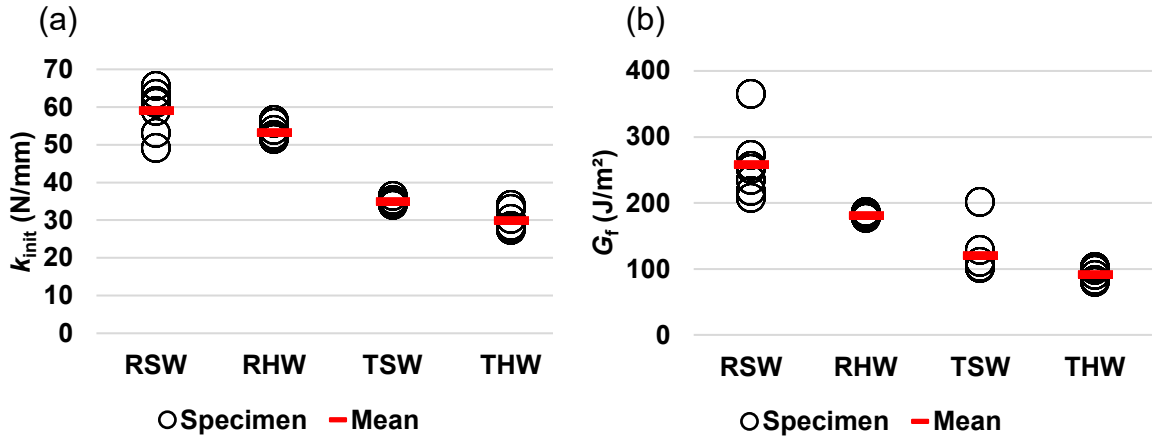

Fig. 3. Single-edge notched bending (SENB) test: (a) Stiffness (k_{init}) and (b) fracture energy (G_f)

ANOVA showed a statistically significant difference among the four treatments tested, with p-values of 1.68 x 10^{-14}, 4.88 x 10^{-09}, 8.23 x 10^{-17}, and 5.03 x 10^{-18} for k_{init}, G_f, P_{max}, and K_{IC}, respectively, indicating highly significant results. After confirming a statistically significant difference via ANOVA, a Tukey test was conducted to identify which groups differed from one another. The Tukey test results are shown in Table 3.

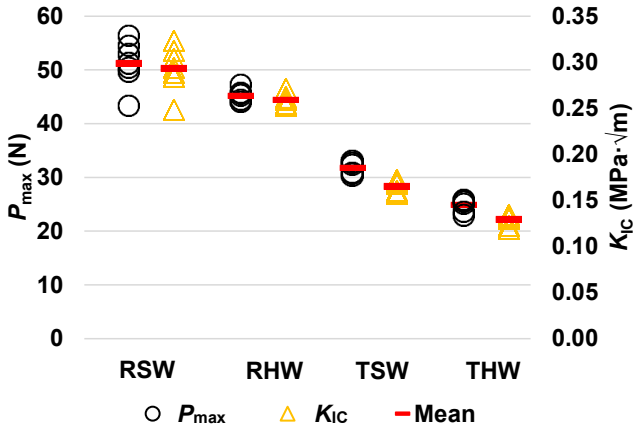

Fig. 4. Single-edge notched bending (SENB) test. Maximum load (P_{max}) and fracture toughness in Mode-I (K_{IC})

Table 3. Tukey Test Results

Specimen Type	Mean Values			
	k_{init} (N/mm)	G_f (J/m^2)	P_{max} (N)	K_{IC} (MPa·m$^{1/2}$)
RSW	59.1 [a]	259 [a]	51.2[a]	0.29 [a]
RHW	53.5 [a]	182 [b]	45.2[b]	0.26 [b]
TSW	35.1 [b]	122 [c]	31.8[c]	0.17 [c]
THW	30.0 [b]	93 [c]	24.9[d]	0.13 [d]

Table 3 shows the mean values for each specimen type in the variables evaluated. The Tukey test results were classified with letters. Treatment conditions having the same letter are statistically equivalent, and different letters mean they are statistically different. For example, for the property k_{init}, RSW and RHW are both classified as "a", meaning that they are statistically equivalent. On the other hand, TSW and THW are classified as "b" meaning they are equivalent to each other (same letter), but both are statistically different from the treatments classified as "a" (RSW and RHW).

From this analysis, it was observed that sapwood and heartwood did not affect the k_{init}, but the system did. Moreover, G_f was statistically different for the RL system (RSW and RHW), but the TL system (TSW and THW) did not show a statistical difference. P_{max} and K_{IC} were the only properties that showed a statistical difference among all the specimen types (treatments). In other words, according to the statistical analysis, they were influenced by sapwood and heartwood, as well as the system.

X-ray CT Analysis

The transverse view showed that in the RL system, the crack propagated in an irregular line, whereas in the TL system, the crack propagated along a straighter line. This resulted in a greater fracture area in the RL system (Fig. 5a). These observations are consistent with the higher G_f results in the RL system obtained in the SENB test.

SEM Analysis

For the RL system specimens, fracture mainly occurred in the earlywood through cell fracture, and the effect of the rays arresting crack propagation was also observed. The fracture surfaces of the RSW specimens were rougher than those of the RHW specimens (Fig. 6). The TL system specimens mainly showed cell separation in latewood and cell fracture in earlywood (Fig. 7). Rays with cell fractures were predominantly observed in the TSW specimens. On the other hand, the THW specimens' rays showed more cell separation than those of the TSW specimens. However, this difference was observed in only two specimens, whereas the other half exhibited a fracture path very similar to that of the TSW specimens.

The specimens showed stable load-displacement curves (Fig. 2), which is a common softwood behavior that was also observed in *P. abies* (Reiterer *et al*. 2002). The RL system exhibited higher values for the evaluated properties, which agree with the results of previous studies.

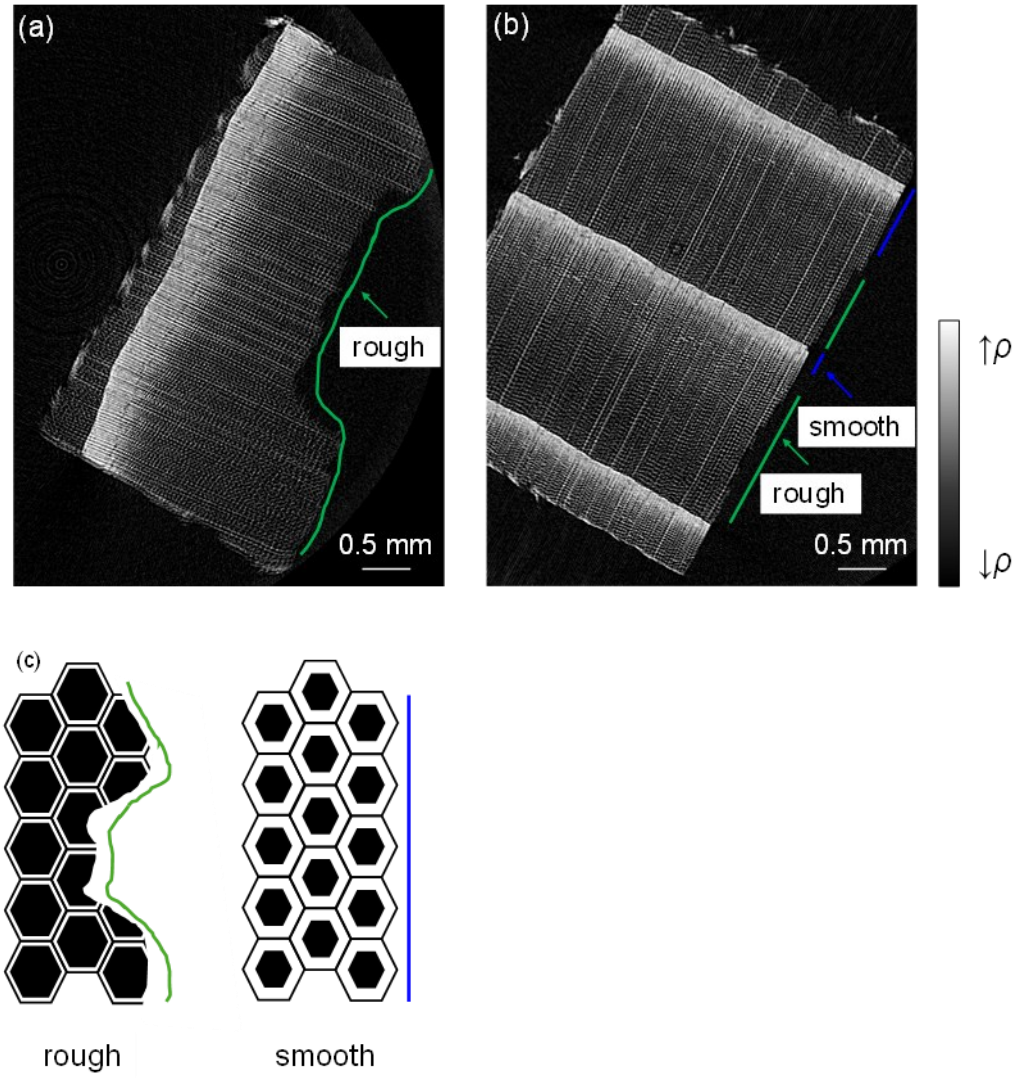

Fig. 5. X-ray computed tomography (CT). Transverse view of (a) radial-longitudinal (RL) and (b) tangential-longitudinal (TL) systems. (c) Schematic illustration of the rough and smooth surface. Fracture surface on the right side. The annotation "↑ρ" indicates higher density and "↓ρ" indicates lower density.

Discussion

X-ray CT analysis showed that the crack propagates in an irregular line in the RL system, creating a greater fracture area compared to the TL system, where the propagation occurred in a straighter line (Fig. 5). Aside from that, in the RL system, the crack only propagates through the earlywood. The earlywood cells are softer compared to latewood cells, enabling more deformation before fracturing. These characteristics contribute to a higher G_f, explaining the higher G_f values in the RL specimens.

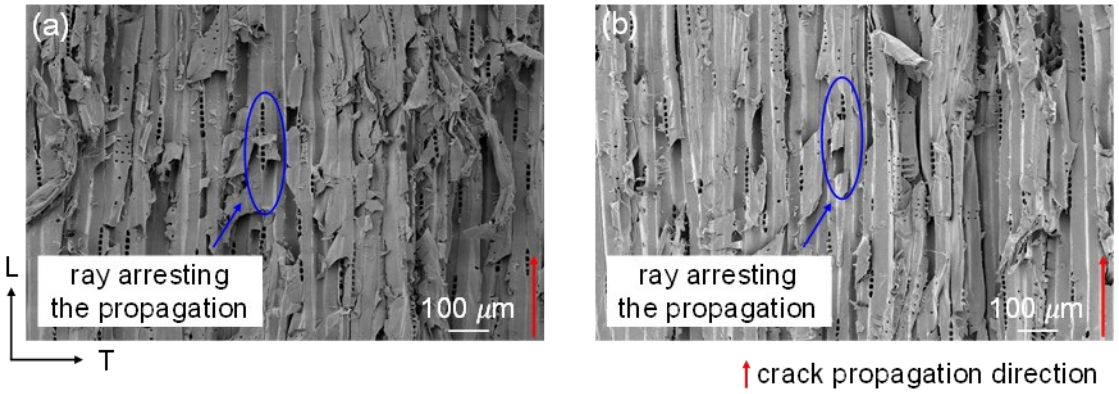

Fig. 6. Characteristic fractures. (a) Radial-longitudinal system for sapwood (RSW) and (b) radial-longitudinal system for heartwood (RHW) specimens

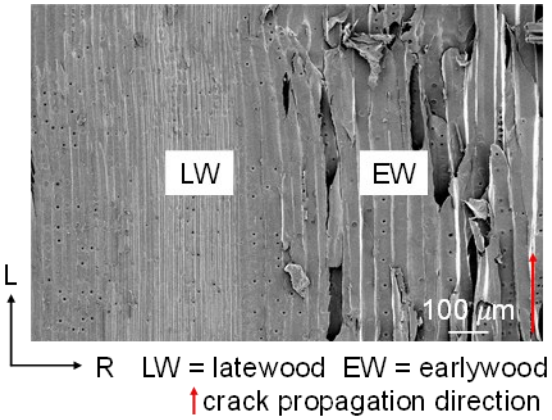

Fig. 7. Characteristic fracture for tangential-longitudinal (TL) system latewood and earlywood

Rough patterns for the RL system (Fig. 6), where fractures occurred only in the earlywood, were observed. The TL system had rough patterns for earlywood and smooth patterns for latewood (Fig. 7), where the actual fracture surface showed more rough patterns than smooth patterns because the specimens had higher earlywood proportions. In cell fracture (Fig. 8a), a crack propagates through the secondary cell wall, resulting in a rough surface. In contrast, cell separation (Fig. 8b) occurs through the middle lamella and primary cell wall, resulting in a smoother surface. Therefore, the results suggested that cell fracture most likely occurred in the RL system and TL earlywood, and cell separation occurred in the TL latewood. Nonetheless, a more detailed analysis was necessary; hence, SEM analysis was performed.

In the SEM analysis, the role of the rays in arresting crack propagation in the RL system (Fig. 6) and their contribution to crack propagation in the TL system were observed. In the RL system, the rays are perpendicular to the crack plane and capable of pulling out or buckling the cells, resulting in more local damage and increasing fracture work. In the

TL system, the rays cause cross-cell failures, such as peeling, which contributes to crack propagation (Boatright and Garrett 1983).

The SEM analysis confirmed that the RL system fracture was mainly caused by cell fracture. In contrast, fractures in the TL system occurred mainly through cell separation in the latewood and cell fracture in the earlywood. The difference between the earlywood and latewood fracture paths may be attributed to cell wall thickness. The thicker latewood cell walls create a higher resistance to microcrack formation (Romanowicz and Grygorczuk 2024), whereas the thin earlywood cells allow the cracks to break through the cell wall more easily (Fig. 9).

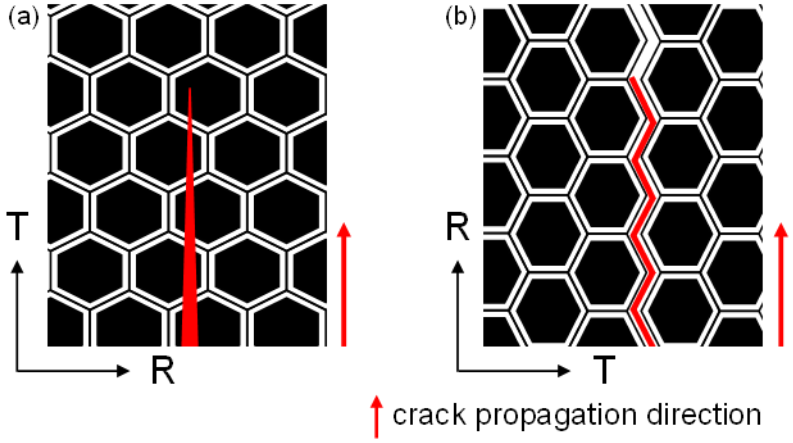

Fig. 8. Fracture path: (a) cell fracture and (b) cell separation

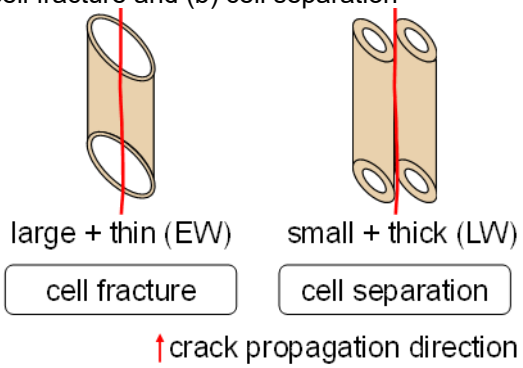

Fig. 9. Earlywood (EW) and latewood (LW) fracture path

Different cell arrangements in the earlywood and latewood may also influence the fracture path. According to FPL (2010), in the softwood transverse section of earlywood, the tracheids have thin walls and are polygonal-shaped, whereas in latewood, they have thicker walls and are flattened radially. For *C. japonica*, this characteristic was observed by Saiki (1982). This may contribute to cell separation in latewood because cracks can propagate directly between cells. On the contrary, in earlywood, cracks propagate by breaking the cell walls because of the more irregular cell arrangement and thinner walls.

Statistical analysis (Table 3) revealed that the k_{init} values from the RL and TL systems were statistically different; however, no significant difference was observed within the same system. Therefore, sapwood and heartwood did not affect this property. Furthermore, the G_f of RSW and RHW were statistically different, contrary to the TSW and THW specimens. This shows that the total energy required in the fracture process was influenced by the sapwood and heartwood in the RL system, but not by that in the TL

system. This result can be due to the higher MC in the THW specimens. The hypothesis is that when the MC increases, the cells become softer, allowing more deformation before the fracture occurs, hence increasing the G_f.

P_{max} and K_{IC} were the only variables in which all specimen types exhibited significant differences, showing that sapwood and heartwood influenced crack initiation and propagation in both systems. These results demonstrate that although the energy required to propagate a crack differed between TSW and THW, their toughness mechanisms were similar. Furthermore, sapwood and heartwood had different effects on k_{init} and G_f values of the RL and TL systems. Considering that the THW specimens had a lower density and higher MC than that of the TSW specimens, the hypothesis was that k_{init} and G_f were more influenced by the density and MC than P_{max} and K_{IC}, which showed a statistical difference for both systems. The results from this study indicated that the density and MC influence the toughness mechanism. Moreover, although specimens with similar densities were selected and stored under the same conditions, the heartwood specimens ended up with higher MC. This is thought to be caused by the presence of extractives in heartwood specimens. This agrees with Bektas *et al*. (2020) statement, where the authors affirm that the differences between sapwood and heartwood physical and mechanical properties need to be considered.

The Wood Handbook (FPL 2010) states that because sapwood and heartwood have equal mechanical properties, they do not need to be considered in stress grading. The k_{init} results supported this statement. Nevertheless, the K_{IC} results in the current study showed that the P_{max} value that each specimen can support before crack initiation was influenced by sapwood and heartwood. According to de Moura *et al*. (2008), fracture mechanics better describes mechanical rupture than the classical strength-of-materials approach does. Thus, the current study showed that understanding sapwood and heartwood fracture mechanisms is important for enhancing the safety of wood structures.

The differences between sapwood and heartwood in both systems were also verified at the microscopic level. The RSW showed more cell fractures than the RHW specimens, resulting in rougher surfaces. For the TL system, the difference was less pronounced, and the TSW specimens showed mainly rays with cell fracture, whereas the THW specimens showed rays with more cell separation. However, this behavior was only observed for half of the THW specimens. Hence, further investigation is necessary. Nevertheless, the subtle differences found among the TL specimens were in agreement with the statistical results, where they only had a significant difference for P_{max} and K_{IC}.

The microscopic analyses showed that the specimens with sapwood (RSW and TSW) exhibited more cell fracture within the same system than those with heartwood (RHW and THW). Therefore, the higher toughness mechanism found for the sapwood specimens was also related to the higher proportion of cell fracture that occurred. Cell fracture has a higher K_{IC} than cell separation. This behavior can be explained by the proportions of cellulose and lignin in the different cellular layers. Because cellulose has a higher K_{IC} than that of lignin and is mainly found in the S_2 layer, cell fracture, which occurs through the secondary cell wall, has a higher K_{IC} than that of cell separation (Conrad *et al*. 2003).

Initially, in wood formation, the cell structure is approximately the same; however, extractives are deposited in the interior layers, over time forming the heartwood. This mechanism explains why some properties, such as the cellulosic structure, are very similar; nevertheless, the filling of the cells' lumens with extractives results in a stiffening effect. The extractives contained in the heartwood make the cells stiffer, allowing less deformation

before the fracture, resulting in a more brittle behavior and lower resistance to crack propagation, which explains why the heartwood specimens showed lower values. Nonetheless, the difference between TSW and THW G_f results was not statistically significant. One of the possible reasons is due to the TL system fracture path. Compared to the RL system, the TL system presents more cell separation, where the crack propagates through the middle lamella and primary cell wall. Since in this fracture path, the crack propagation does not go through the cell lumen, the extractives' influence is less pronounced.

As for the RL system, aside from the rays arresting the crack propagation, a greater fracture area, and the main fracture path being cell fracture, in this system, the crack only propagates through the earlywood. The earlywood cells are softer than the latewood cells, allowing more deformation before fracturing. The combination of these factors results in RSW having the greatest resistance to fracture among all the specimen types.

While this study confirmed the influence of sapwood and heartwood on *C. japonica* toughness mechanism, further research is necessary to understand their influence on fracture mechanics. Therefore, future studies will explore their influence on FPZ development.

CONCLUSIONS

The influence of the chemical composition of sapwood and heartwood on the *C. japonica* radial-longitudinal (RL) and tangential-longitudinal (TL) systems in mode-I was investigated using the single-edge notched bending (SENB) test, X-ray computed tomography (CT), and scanning electron microscopy (SEM) analysis. To ensure a reliable comparison between sapwood and heartwood, mature and clear wood was used, and specimens with similar density and moisture content (MC) were selected. The main conclusions are the following:

1. Statistical analysis showed that the stiffness (k_{init}) was affected by the change in the direction perpendicular to the crack plane but was not influenced by sapwood and heartwood.
2. The TL system G_f was statistically equivalent; however, the TSW and THW P_{max} and K_{IC} were significantly different, indicating that the toughness mechanism was similar in the TL system. Nevertheless, the energy required to propagate the crack (K_{IC}) differed for sapwood and heartwood.
3. In the SEM analysis, sapwood and heartwood fracture differences were more pronounced in the RL system, where RSW showed more cell fractures than those of RHW. In the TL system, half of the THW specimens exhibited rays with more cell separation than in the TSW system. Hence, microscopic analyses revealed that the higher toughness mechanism in the sapwood was related to the higher cell fracture proportion found in the sapwood specimens.
4. The heartwood extractives are believed to stiffen the cells, allowing for less deformation and resulting in lower resistance to crack propagation. Moreover, the heartwood influence was more pronounced in specimens that presented more cell fracture.

ACKNOWLEDGMENTS

This research was supported by JSPS KAKENHI (grant number 24K09020). The authors express their deepest gratitude to Professors Hiroshi Yoshihara, Yutaka Sawada, and Yoshiyuki Yanase for their support during the study. Special thanks go to the Ministry of Education, Culture, Sports, Science and Technology (MEXT) of Japan for granting the first author's scholarship.

Authors' Contributions

T.M.E. performed the experiments (SENB test, X-ray CT, SEM analysis), data analysis, and writing (original draft, review, and editing). A.Y. supported the SEM analysis and discussion. N.Y. provided specimens and advice. K.M. performed the experiments (SENB test, X-ray CT), supervised discussions, and conducted reviews. All the authors have read and approved the final manuscript.

Availability of Data and Materials

The data that support the findings of this study are available from the corresponding author, T. M. E., upon reasonable request.

Competing Interests

The authors declare that they have no competing interests.

Partial contents of this study were presented at the ISWST (International Symposium on Wood Science and Technology) held on March 17~19, 2025 - Sendai, Japan. This manuscript has not been published and is not being considered for publication elsewhere. All the authors have read the manuscript and approved this submission.

REFERENCES CITED

Bektaş, İ., Tutuş, A., and Gültekin, G. (2020). "The effect of sapwood and heartwood differences on mechanical properties of fast-growing tree species," *Drvna Ind.* 71(3), 261-269. https://doi.org/10.5552/drvind.2020.1940

Bertaud, F., and Holmbom, B. (2004). "Chemical composition of earlywood and latewood in Norway spruce heartwood, sapwood and transition zone wood," *Wood Sci. Technol.* 38, 245-256. https://doi.org/10.1007/s00226-004-0241-9

Boatright, S. W. J., and Garrett, G. G. (1983). "The effect of microstructure and stress state on the fracture behaviour of wood," *J. Mater. Sci.* 18, 2181-2199. https://doi.org/10.1007/BF00555013

Conrad, M. P. C., Smith, G. D., and Goran, F. (2003). "Fracture of solid wood: A review of structure and properties at different length scales," *Wood Fiber Sci.* 35 (4), 570-584.

Fonselius, M., and Riipola, K. (1992). "Determination of fracture toughness for wood," *J. Struct. Eng.* 118 (7), 1727-1740. https://doi.org/10.1061/(ASCE)0733-9445(1992)118:7(1727)

Forest Products Laboratory (FPL) (2010). *Wood Handbook: Wood as an Engineering Material*, Madison, WI, USA.

Frühmann, K., Reiterer, A., Tschegg, E. K., and Stanzl-Tschegg, S. S. (2002). "Fracture characteristics of wood under mode I, mode II and mode III loading," *Philos. Mag.* 82

(17-18), 3289-3298. https://doi.org/10.1080/01418610208240441
Jeronimidis, G. (1980). "The fracture behaviour of wood and the relations between toughness and morphology," *P. R. Soc. London* 208, 447-460. https://doi.org/10.1098/rspb.1980.0062
Majano-Majano, A., Hughes, M., and Fernandez-Cabo, J. L. (2012). "The fracture toughness and properties of thermally modified beech and ash at different moisture contents," *Wood Sci. Technol.* 46, 5-21. DOI: 10.1007/s00226-010-0389-4
Majano-Majano, A., Lara-Bocanegra, A. J., Xavier, J., and Morais, J. (2018). "Measuring the cohesive law in mode I loading of *Eucalyptus globulus*," *Materials* 12(1), 1-14. https://doi.org/10.3390/ma12010023
Matsumoto, N., and Nairn, J. A. (2012). "Fracture toughness of wood and wood composites during crack propagation," *Wood Fiber Sci.* 44 (2), 121-133.
Merela, M., and Čufar, K. (2013). "Mechanical properties of sapwood versus heartwood, in three different oak species," *Drvna Ind.* 64 (4), 323-334. https://doi.org/10.5552/drind.2013.1325
Merhar, M., Pitti, R. M., and Argensse, T. (2023). "Mode I fracture properties of thermally-modified spruce wood (*Picea abies*) at different moisture contents," *Wood Mater. Sci. Eng.* 18 (6), 2093-2103. DOI: 10.1080/17480272.2023.2228280
de Moura, M. F. S. F., Morais, J. J. L., and Dourado, N. (2008). "A new data reduction scheme for mode I wood fracture characterization using the double cantilever beam test," *Eng. Fract. Mech.* 75 (13), 3852-3865. https://doi.org/10.1016/j.engfracmech.2008.02.006
Özden, S., Ennos, A. R., and Cattaneo, M. E. G. V. (2017). "Transverse fracture properties of green wood and the anatomy of six temperate tree species," *Forestry* 90 (1), 58-69. https://doi.org/10.1093/forestry/cpw023
Ozyhar, T., Hering, S., and Niemz, P. (2012). "Moisture-dependent elastic and strength anisotropy of European beech wood in tension," *J. Mater. Sci.* 47 (16), 6141-6150. https://doi.org/10.1007/s10853-012-6534-8
Pietropaoli, E. (2011). "Virtual crack closure technique and finite element method for predicting the delamination growth initiation in composite structures," in: *Advances in Composite Materials - Analysis of Natural and Man-Made Materials*, P. Tesinova (ed.), Rijeka, Croatia, pp. 463-480.
Reiterer, A., Sinn, G., and Stanzl-Tschegg, S. E. (2002). "Fracture characteristics of different wood species under mode I loading perpendicular to the grain," *Mater. Sci. Eng.* 332, 29-36. https://doi.org/10.1016/S0921-5093(01)01721-X
Rybicki, E. F., and Kanninen, M. F. (1977). "A finite element calculation of stress intensity factors by a modified crack closure integral," *Eng. Fract. Mech.* 9 (4), 931-938. https://doi.org/10.1016/0013-7944(77)90013-3
Romanowicz, M., and Grygorczuk, M. (2024). "The effect of crack orientation on the mode I fracture resistance of pinewood," *Int. J. Fracture* 248, 27-48. https://doi.org/10.1007/s10704-024-00798-z
Saiki, H. (1982). *The Structure of Domestic and Imported Woods in Japan*, Japan Forest Technical Association, Tokyo, Japan. In Japanese.
Sawada, M. (1963). "Elasticity and strength of wood as an orthotropic material," *J. Soc. Mater Sci, Japan* 12 (121), 73-77. https://doi.org/10.2472/jsms.12.749
Sih, G. C., Paris, P. C., Irwin, G. R. (1965). "On cracks in rectilinearly anisotropic bodies," *Int. J. Fracture* 1(3), 189-203. https://doi.org/10.1007/bf00186854

Smith, I., Landis, E., and Gong, M. (2003). *Fracture and Fatigue in Wood*, John Wiley & Sons Ltd., Chichester, England.

Song, K., Yin, Y., Salmén, L., Xiao, F., and Jiang, X. (2014). "Changes in the properties of wood cell walls during the transformation from sapwood to heartwood," *J. Mater. Sci.* 49, 1734-1742. https://doi.org/10.1007/s10853-013-7860-1

Xie, D., Wass, A. M., Shahwan, K. W., Schroeder, J. A., and Boeman, R. G. (2004). "Computation of energy release rates for kinking cracks based on virtual crack closure technique," *CMES-COMP MODEL ENG* 6 (6), 515-524. https://doi.org/10.3970/CMES.2004.006.515

Article submitted: September 9, 2025; Peer review completed: October 5, 2025; Revised version received: March 3, 2026; Accepted: March 4, 2026; Published: March 12, 2026.
DOI: 10.15376/biores.21.2.3894-3909

APPENDIX

Table A1. List of Abbreviations

Abbreviation	Meaning
ANOVA	analysis of variance
CT	computed tomography
FEA	finite element analysis
G_f	fracture energy
K_{IC}	fracture toughness in mode-I
k_{init}	stiffness
MC	moisture content
MFA	microfibril angle
P_{max}	maximum load
RHW	radial-longitudinal system for heartwood
RL	radial-longitudinal
RSW	radial-longitudinal system for sapwood
SEM	scanning electron microscopy
SENB	single-edge notched bending
THW	tangential-longitudinal system for heartwood
TL	tangential-longitudinal
TSW	tangential-longitudinal system for sapwood
VCCT	virtual crack closure technique

Table A2. Tukey Test Mean Significant Difference

Comparison		k_{init}		G_f		P_{max}		K_{IC}	
		MD	**MSD**	**MD**	**MSD**	**MD**	**MSD**	**MD**	**MSD**
RSW	**RHW**	5.61	6.36	76.29	60.11	5.99	4.31	0.03	0.02
RSW	**TSW**	23.99		137.23		19.39		0.13	
RSW	**THW**	29.15		165.73		26.29		0.16	
RHW	**TSW**	18.38		60.93		13.40		0.09	
RHW	**THW**	23.54		89.44		20.30		0.13	
TSW	**THW**	5.16		28.50		6.90		0.04	

Note: MD is the mean difference, MSD is the mean significant difference